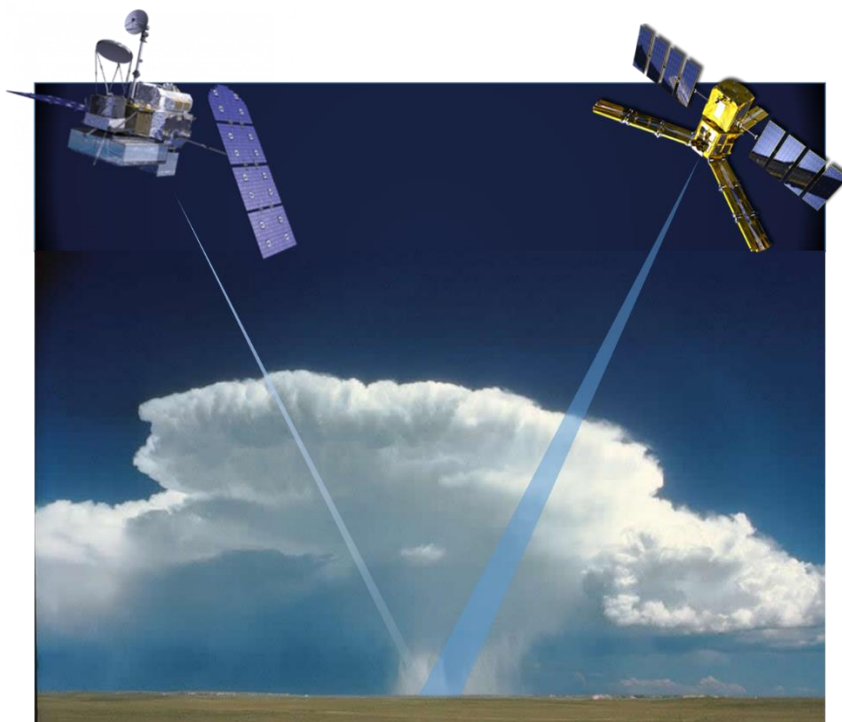# The PrISM*

# precipitation product

## *Precipitation Inferred from Soil Moisture

Author : T. Pellarin

29/08/2018

# Table of contents

## 1.   The concept of the PrISM Product

The concept of the PrISM (Precipitation Inferred from Soil Moisture) product is to exploit remote sensing soil moisture measurements to correct for a satellite-based rainfall product. As soil moisture can be seen as the trace of the precipitation, some research teams in US, France and Italy started to develop various algorithms to retrieve rainfall from soil moisture measurements based on in-situ or satellite soil moisture measurements (Crow et al, 2007, 2009, Pellarin et al., 2009, 2013, Brocca et al. 2013; 2014, Wanders et al. 2015, Zhan et al. 2015). The present methodology (PrISM) makes used of a simple land-surface model associated to an assimilation scheme (Particle Filter). The land-surface model is used to generate a first-guess soil moisture time-series based on a given satellite precipitation product. Then, this soil moisture time-series is compared to a satellite soil moisture product. The concept of the PrISM methodology is to exploit the difference between the two time-series by increasing or decreasing the amount of water of the original satellite precipitation product. The methodology is able to provide an unbiased real-time precipitation product based on the correction of a raw satellite-based precipitation product.

In its present form, the PrISM product is proposed on the continental Africa for two main reasons. First, there is a significant need for precipitation measurements in Africa that are not provided by traditional ground-based measurement technics due to the absence of weather radars and the low density of the rain gauge network (about 1 rain gauge for 10 000 km²). Second, the identified limitations of the PrISM methodology were found to be related to snow cover and strong topography, land surface conditions not often encountered in Africa.

## 2.   The API model

The API (Antecedent Precipitation Index) model is based on a small modification of the original API model, presented in Pellarin et al. (2013). The original version of the API produces an index of the soil moisture expressed in mm. The new version of the API model contains two modifications: (i) it accounts for the degree of saturation of the soil before a rain event; and (ii) the soil moisture is now expressed in $m^3/m^3$. These modifications of the relationship add three parameters ($d_{soil}$: an equivalent soil thickness (in mm), $\theta_{sat}$: the soil moisture value at saturation (in $m^3/m^3$) and $\theta_{res}$ the residual soil moisture (in $m^3/m^3$)). This simple model is expressed as follows:

$$\theta_{(t)} = \left(\theta_{(t-1)} - \theta_{res}\right).e^{-\frac{\Delta t}{\tau}} + \left(\theta_{sat} - \left(\theta_{(t-1)} - \theta_{res}\right)\right).\left(1 - e^{\frac{-P(t)}{dsoil}}\right) + \theta_{res} \qquad \text{(Eq.1)}$$

where $\tau$ is the soil moisture drying-out velocity (in h), $\theta(t)$ is the surface soil moisture in $m^3/m^3$, and $P(t)$ is the cumulative precipitation in mm during the $\Delta t$ period. It is required to use a precipitation product at infra-daily resolution (3 hours or less) to determine when the rainfall occurs compared to SMOS ascending (6am) or descending (6pm) orbits. A sensitivity study was conducted over the 10 sites at the global scale (Román-Cascón et al., 2017) to derive the best 4 parameters of the API model. and showed that a constant value for $\theta_{sat}$ = 0.45 $m^3/m^3$ provided reliable results. On the contrary, it was shown that the $\tau$ and $d_{soil}$ values have to be spatially and temporally defined (see section 0).

## 3.   The Particle Filter assimilation scheme

The selected assimilation scheme is the Particle Filter (PF). The PF is an original method based on stochastic perturbations of the precipitation forcing that explicitly simulates the consequence of these uncertainties in the associated output, i.e., the soil moisture (Doucet et al., 2000;  Moradkhani et al., 2005; Van Leeuwen, 2009). It is suitable for non-linear models and makes no assumptions on the prior and posterior distributions of the model states. This property of the PF makes it more suitable for this study compared to ensemble based data assimilation approaches whose optimality and performance depend on the linearity between input and output variables, having Gaussian distributed errors, as for example in the Ensemble Kalman Filter (Evensen, 2003; Reichle 2008). An illustration of the PF assimilation method is shown in Figure 1 (Niger site, 2015).
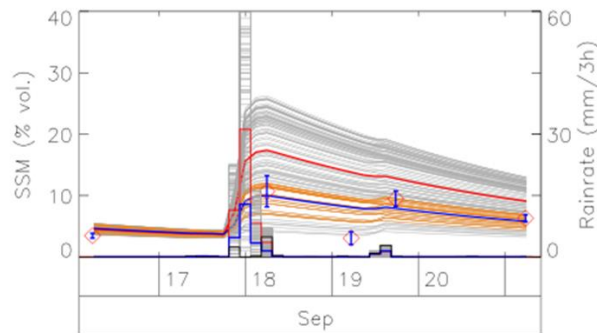


*Figure 1: Illustration of the PF assimilation scheme. The initial precipitation rate (in red) produces the associated soil moisture (in red). Stochastic perturbations of the initial precipitation product produce an ensemble of potential soil moisture evolutions (in grey). The SMOS measurements (diamonds) are used to select the most probable soil moisture curves (in orange) and to calculate the averaged soil*

## 4. Pre-Processing steps

The methodology requires four preliminary successive steps:

1. Select a reference precipitation product (we used the 2012 CMORPH-adjusted).

2. Read the required parameters for the API model ($\tau$(x,y,t), $H_{soil}$(x,y), $\theta_{sat}$ and $\theta_{res}$). These parameters were determined using *in situ* soil moisture measurements over 10 sites located in US, Europe, Africa and Australia (see section 1.4)

3. Run the API model for 2012 year.

4. Read the SMOS soil moisture measurements and their associated quality scores (RFI(x,y,t), Dqx(x,y,t), Chi2(x,y,t)) and calculate the two CDF-matching coefficient maps (p1(x,y) and p2(x,y)) to get unbiased SMOS measurements. This re-scaling step makes comparable the API soil moisture simulations and the SMOS soil moisture observations.
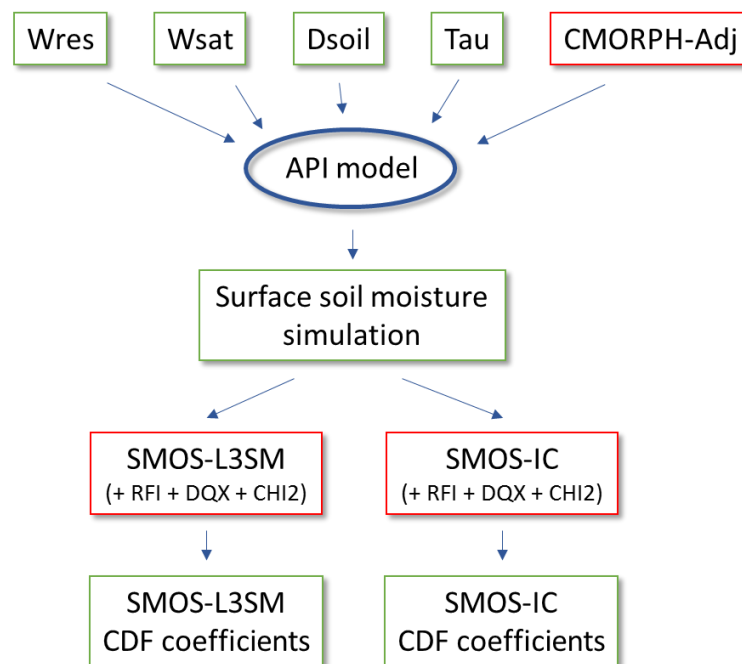


*Figure 2: Processing steps required to implement the PrISM algorithm. The upper part of the chart is common to all satellite soil moisture products. The lower part of the chart (CDF-matching coefficient calculation) depends on the selected soil moisture product (SMOS-L3SM or SMOS-IC in this example).*

## 5. PrISM algorithm

The PrISM algorithm is illustrated in Figure 3 and can be described as followed. When a SMOS measurement is available on a given pixel, the PrISM method determines an assimilation period fixed to 5 SMOS measurements (~4-6 preceding days). Then, a stochastic perturbations (100) of the original precipitation forcing is performed at the rain event time-scale. The API model (Eq. 1) simulates the 100

potential soil moisture trajectories. The re-scaled SMOS measurements (diamonds in Figure 3) are used to select the most probable soil moisture trajectories (in orange, lower RMSE scores) and calculate the averaged soil moisture (in blue), which is associated with a specific precipitation rate (in blue). On the first graph of Figure 3a, it can be observed that the original rainfall event (in red) is overestimated in comparison with in situ rainfall measurements (in black). However, at this stage, an increase of the rainfall rate is proposed by the PrIMS algorithm (in blue). The process is repeated when a new SMOS measurement is available (Figure 3b). Here, the PrIMS algorithm revises downward the proposed rainfall rate for the same event due to a new SMOS soil moisture measurement. The same process is repeated for the next two SMOS measurements as shown in Figure 3c and Figure 3d. At the end, each rainfall event is observed 4 times (a period of 5 successive SMOS measurements provides 4 intervals) and the final rainfall rate correction is the average value of the 4 proposed rainfall rate. At the end of the process, for the specific rainfall event of 11-12 September 2015 in Niger, the *in situ* rainfall amount was 15 mm whereas the original rainfall was 29 mm (CMORPH-Raw) and the PrISM rainfall was evaluated to 22 mm.
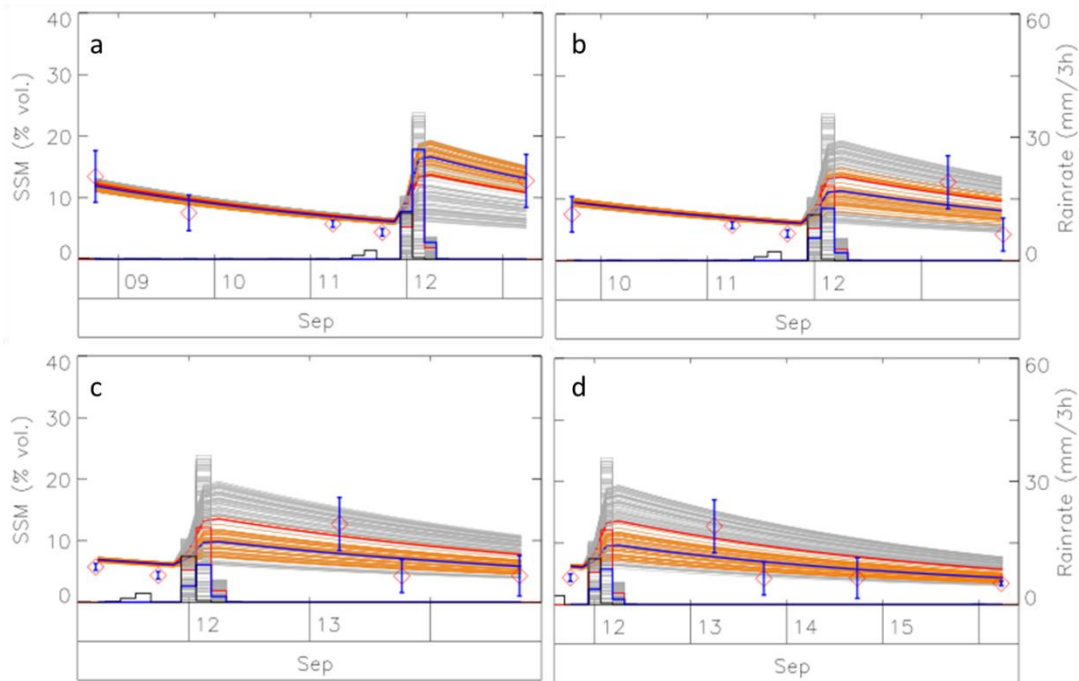


*Figure 3: PrISM successive assimilation steps to derive a rainfall estimation. When a SMOS measurement is available, the PrISM method considers the preceding period (fixed to 5 SMOS measurements, ~4-6 days), and the algorithm select the best precipitation modification that minimize the RMSE between SMOS (measurements) and API (simulations) soil moisture.*

## 6.    Evaluation at the local scale

The spatial resolution of the PrISM product is fixed by the precipitation product to be corrected (0.25° for CMORPH, TRMM and PERSIANN). At this scale, a comparison of the PrISM product with a single raingauge station at the ground level might be biased or inaccurate. Thus, we used two AMMA-CATCH observatory sites located in Niger and in Benin which contains two high density raingauge networks composed (depending on years) between 4 to 24 raingauge stations over the two 0.25° considered pixels. The center coordinates of the two areas are: 13.625°N; 2.625°E (Niger) and 9.625°N; 1.625°E

(Benin). On the two sites, a block-krigging technique was carried out using all raingages in the neighborhood of the 0.25° area. It results a rainfall value obtained every 3 hours on the 0.25° x 0.25° area.

A first evaluation of the PrISM product was done on the cumulative annual rainfall for the Niger and Benin sites from 2010 to 2016. *Figure 4* shows the cumulative annual rainfall estimates from (i) in situ measurements, (ii) the PrISM product, (iii) the CMORPH-Raw and CMORPH-Adj products and (iv) the GPCC product. Note that the four first products are 0.25° spatial resolution whereas the GPCC product is a 1° resolution product. The addition of the GPCC product in this section is useful to understand the next section (regional scale evaluation). Results presented in *Figure 4* show that the PrISM product provides accurate cumulative rainfall close to the reference product and always better values that the CMORPH-Raw product. Compared to CMORPH-Adj, which use ground stations to remove the bias at a monthly timescale, the PrISM product provides better cumulative annual rainfall each year in Benin, and 4 years out of 7 in Niger. The mean annual absolute difference in Benin is 62 mm/year with the PrISM product whereas it is 228 mm/year with CMORPH-Adj product (and 392 mm/year with CMORPH-Raw). In Niger, the mean annual absolute difference is 69 mm/year with the PrISM product and 68 mm/year (slightly better) with the CMORPH-Adj product (and 295 mm/year with CMORPH-Raw). Globally, the PrISM product provides better results than GPCC except in 2011 and 2014 in Niger and in 2013 in Benin.
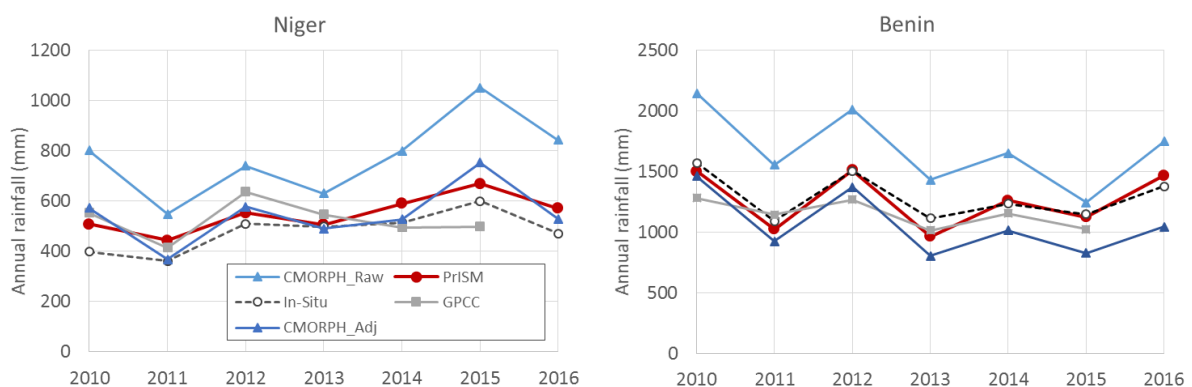


*Figure 4: Annual cumulative rainfall from 2010 to 2016 in Niger (left graph) and Benin (right graph) estimated with in situ raingages (black dotted curve), CMORPH-Raw and CMORPH-Adj products (blue curves, triangle), the PrISM product (red curves) and GPCC product (grey curves, square).*

The PrISM product was also assessed using the correlation (R²) and RMSE scores. *Figure 5* shows the correlation between in situ rainfall (daily timestep) and four products (PrISM, CMORPH-Raw, CMORPH-Adj and GPCC). The PrIMS product improves the correlation scores of the original rainfall product (CMORPH-Raw, here) for 100% of the years on the two sites. More remarkable, the performances of the PrISM product surpasses the CMORPH-Adj product except for one year in Niger (2013). The low correlation scores of the GPCC product are probably due to the different spatial resolution (1° vs. 0.25°), but also to the low spatial variability of this product based exclusively on in situ rainfall network which is known to be sparse in Africa. Similarly, *Figure 6* shows the root-mean-square-error (RMSE) scores between in situ rainfall (daily timestep) and the four products. Here again, the PrIMS product srongly improves the RMSE scores of the original rainfall product (CMORPH-Raw) for 100% of the years on the two sites. When comparing with the CMORPH-Adj product, the PrISM product provides better RMSE scores except in one year in Benin (2016).
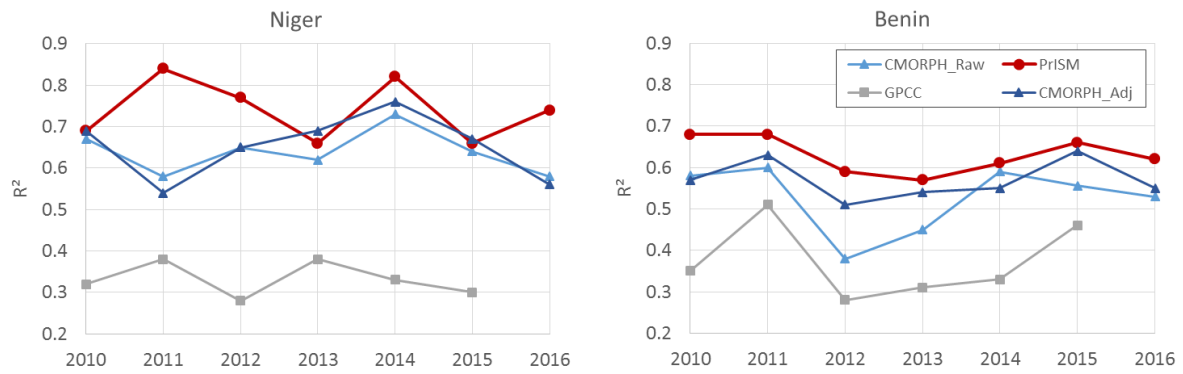
*Figure 5: Annual correlation (R², daily timestep) between in situ raingages vs. (i) CMORPH-Raw and CMORPH-Adj products (blue curves), (ii) vs PrISM product (red curves) and (iii) GPCC. Niger 0.25° pixel (left) and Benin 0.25° pixel (right)*
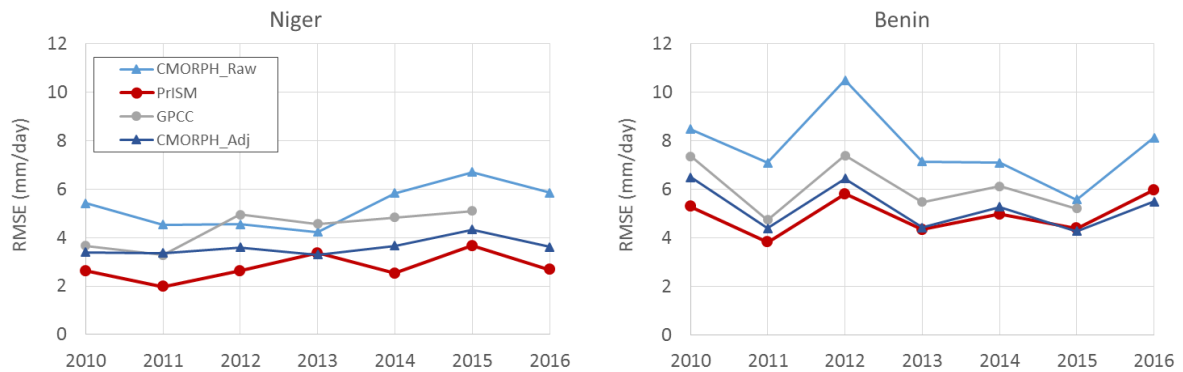


*Figure 6: RMS error (mm/day) between in situ raingages vs. (i) CMORPH-Raw and CMORPH-Adj products (blue curves), (ii) vs PrISM product (red curves) and (iii) GPCC. Niger 0.25° pixel (left) and Benin 0.25° pixel (right)*

## 7.   Evaluation at the regional scale (2015)

The PrISM product was also assessed at the regional scale using GPCC as a reference product. The relevance of the GPCC product as a reference product can be discussed regarding the previous section (1.5) but this product is frequently used for satellite product evaluations and is considered as one of the best precipitation product.

Similarly to previous section, the correlation, the RMSE and the cumulative annual rainfall were calculated and compared to GPCC product. Figure 7 shows the RMSE score (mm/day) for CMORPH-Raw and PrISM products (two first graphs), and the potential improvement/worsening of the PrISM product compared to the CMORPH-Raw product. The two first graphs of Figure 7 shows that larger errors are located in the central part of Africa but this is mostly due to large rainfall amounts in this region compared to northern and southern African regions. The right graph presents the locations where the PrISM product provides better (in blue) or lower (in red) RMSE scores compared to CMORPH-Raw product. In 94% of the pixels, the PrISM product improves the CMORPH-Raw product.
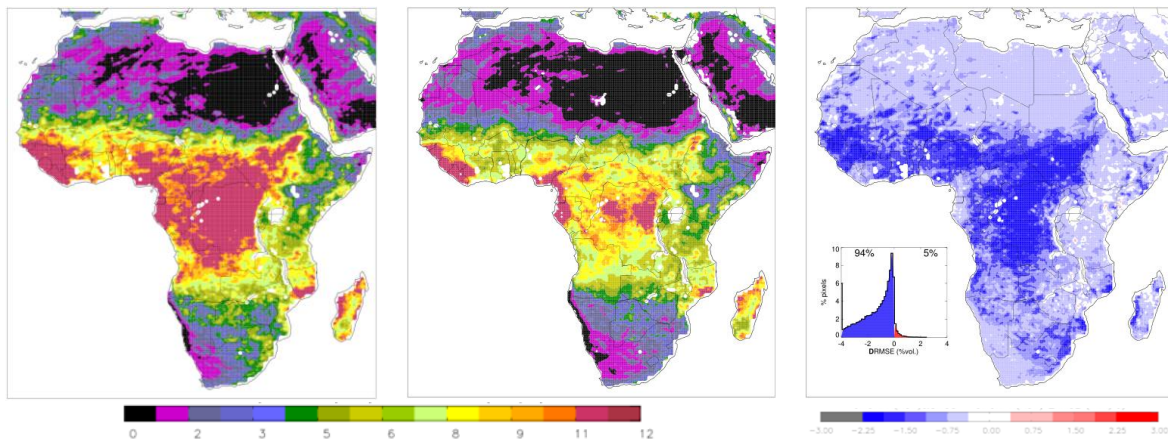
Figure 7: (left) RMSE (mm/day) between GPCC and CMORPH-Raw product, (middle) RMSE between GPCC and PrIMS product and (right) improvement (blue) or worsening (red) of the RMSE score from CMORPH-Raw product to PrISM product.

Similar analysis was done with the correlation score (R²) in Figure 8. The low values of R² of the two first graphs are mainly due to the uncertain correlation score of the GPCC product compared to in situ rainfall (shown in previous section in two sites). Despite this, it can be observed that the PrISM product improve the correlation on 73% of the pixels.
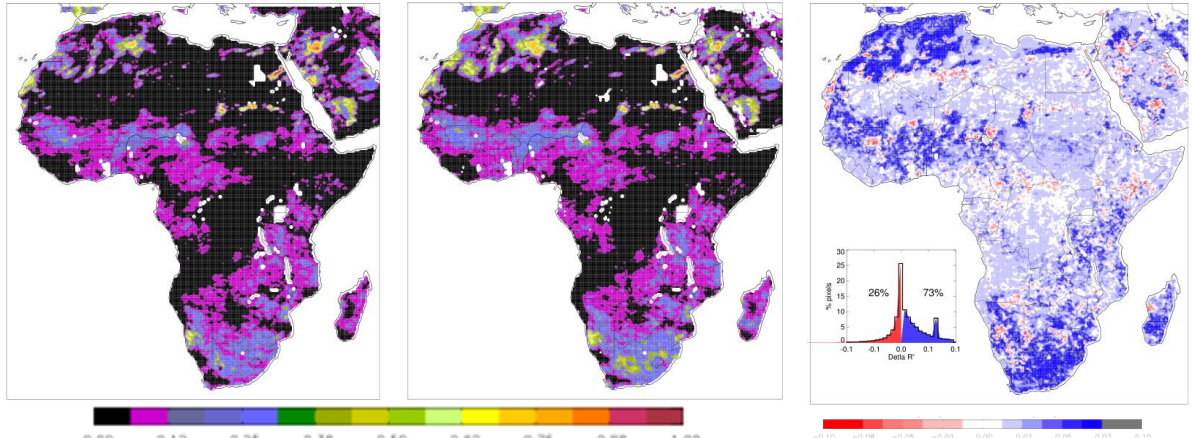


Figure 8: (a) Coefficient of determination (R²) between daily GPCC and daily CMORPH-Raw products, (b) R² between GPCC and the PrISM product and (c) improvement (blue) or worsening (red) of the CMORPH-Raw product compared to GPCC.

Finally, the performance of the PrISM product was evaluated against cumulative annual rainfall. The left graph of

Figure 9 shows that the CMORPH-Raw product tends to overestimate rainfall (blue pixels) on most of Africa (except East Africa, Madagascar, Gabon and Liberia). This middle graph shows the annual difference of the PrISM product compared to GPCC. It can be observed that white and light pixels are more frequent which means that the absolute difference (between PrISM and GPCC) is lower (than CMORPH-Raw). The right graph shows the pixel where the PrISM product provides better (in blue) or lower (in red) RMSE scores compared to CMORPH-Raw product. In 63% of the pixels, the PrISM product

improves the CMORPH-Raw product. Regions where the PrISM product seems to be in difficulty are located in highly dense forest (Liberia, Southern Nigeria, Gabon, Cameroun), and in various locations in East and South Africa. However, the GPCC product is probably not very accurate in these regions as the number of stations used by GPCC are close to zero as shown in Figure 10. Further investigation in these forested regions are on-going.
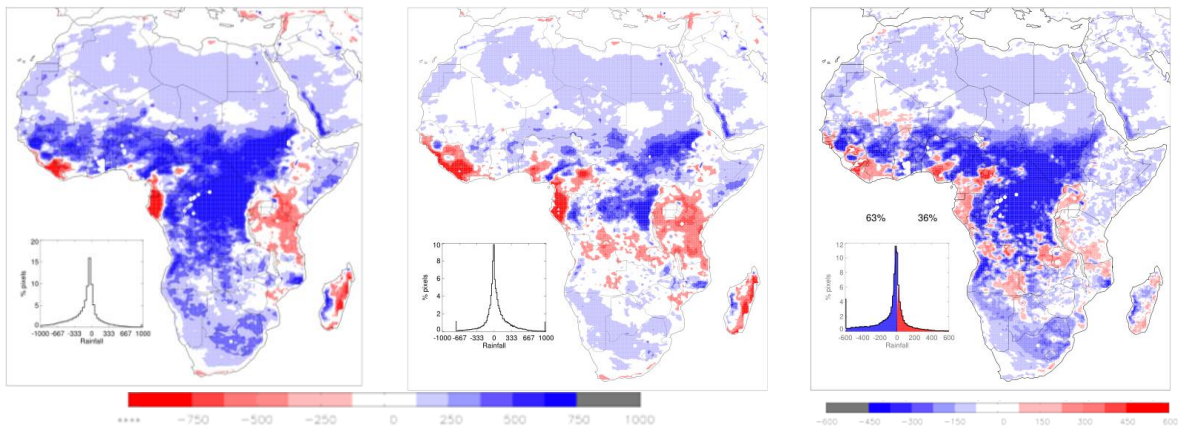


Figure 9: Over (blue) and under (red) estimation of the cumulative annual rainfall compared to GPCC. Left graph refers to CMORPH-Raw, middle graph to PrISM. The right graph shows where the PrISM product is better than CMORPH-Raw (blue) compared to the GPCC annual rainfall and, respectively where the PrISM product is lower (red pixels). Globally, over 63% of the area, the PrISM product provides better annual rainfall than CMORPH-Raw product.
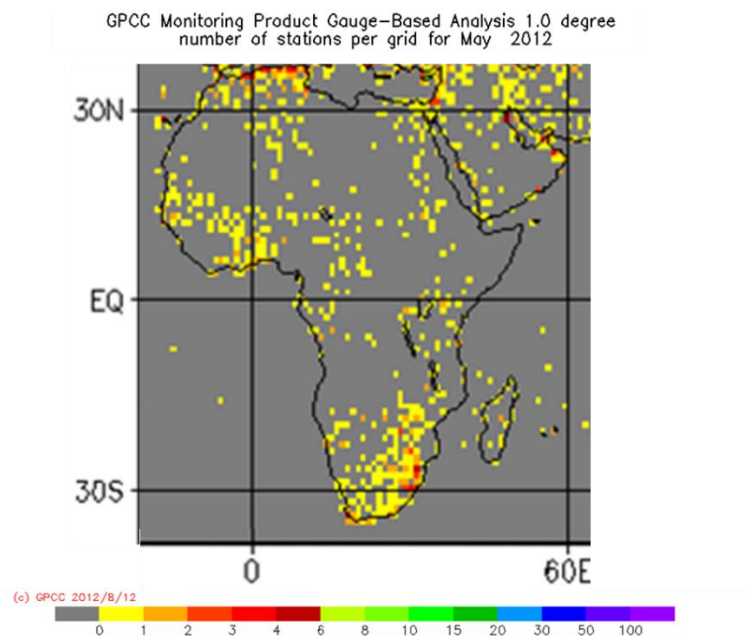


Figure 10: Number of stations used by GPCC for May 2012.

# 8. References

Brocca, L., Ciabatta, L., Massari, C., Moramarco, T., Hahn, S., Hasenauer, S., Kidd, R., Dorigo, W., Wagner, W., & Levizzani, V. Soil as a natural rain gauge: Estimating global rainfall from satellite soil moisture data. Journal of Geophysical Research-Atmospheres, 2014, 119, 5128-5141.

Brocca, L., Moramarco, T., Melone, F., & Wagner, W. A new method for rainfall estimation through soil moisture observations. Geophysical Research Letters, 2013 40, 853-858.

Crow, W.T., & Bolten, J.D.: Estimating precipitation errors using spaceborne surface soil moisture retrievals. Geophysical Research Letters, 2007 ,34

Crow, W.T., Huffman, G.J., Bindlish, R., & Jackson, T.J.: Improving Satellite-Based Rainfall Accumulation Estimates Using Spaceborne Surface Soil Moisture Retrievals. Journal of Hydrometeorology, 2009, 10, 199-212

Doucet, A., Godsill, S., & Andrieu, C.: On sequential Monte Carlo sampling methods for Bayesian filtering. Statistics and Computing, 2000 ,10, 197–208.

Evensen, G.: The ensemble kalman filter: Theoretical formulation and practical implementation. Ocean Dynamics, 2003, 53, 343–367.

Moradkhani, H., Hsu, K. -L., Gupta, H., & Sorooshian, S.: Uncertainty assessment of hydrologic model states and parameters: Sequential data assimilation using the particle filter. Water Resources Research, 2005, 41, W05012. http://dx.doi.org/10.1029/2004WR003604.

Pellarin, T., Tran, T., Cohard, J.M., Galle, S., Laurent, J.P., de Rosnay, P., & Vischel, T: Soil moisture mapping over West Africa with a 30-min temporal resolution using AMSR-E observations and a satellite-based rainfall product. Hydrology and Earth System Sciences, 2009,13, 1887-1896

Pellarin T., S. Louvet, C. Gruhier, G. Quantin, C. Legout, 2013: A simple and effective method for correcting soil moisture and precipitation estimates using AMSR-E measurements, Remote Sensing of Environment, 136, 28–36.

Reichle, R. H: Data assimilation methods in the Earth sciences. Advances in Water Resources, 2008,31, 1411–1418.

Román-Cascón, C., Pellarin, T., Gibon, F., Brocca, L., Cosme, E., Crow, W., ... & Massari, C. (2017). Correcting satellite-based precipitation products through SMOS soil moisture data assimilation in two land-surface models of different complexity: API and SURFEX. Remote Sensing of Environment, 200, 295-310.

Van Leeuwen, P. J. Particle filtering in geophysical systems. Monthly Weather Review, 137(12), 2009, 4089–4114.

Wanders, N., Pan, M., & Wood, E.F. (2015). Correction of real-time satellite precipitation with multi-sensor satellite observations of land surface variables. Remote Sensing of Environment, 160, 206-221

Zhan, W., Pan, M., Wanders, N., & Wood, E.F. (2015). Correction of real-time satellite precipitation with satellite soil moisture observations. Hydrology and Earth System Sciences, 19, 4275-4291

# ANNEX 1 : PrISM's parameters estimation

## a) Seasonal variation of Tau parameter

In the API model (Eq.1), the Tau parameter (τ) describes the drying-out velocity of the surface soil moisture due to both evapotranspiration and infiltration rate. Consequently, the value of this parameter should mainly depends on atmospheric forcing (air temperature, wind velocity, solar radiation) and on the soil hydraulic properties. In a first approximation, it was shown that the τ value can be appropriately estimated only with 30-days smoothed air temperature ($T_{air}$) using the following relationship:

$$\tau(t) = 400 - \left( \frac{350}{(1 + e^{-0.1(Tair - 7.5)})} \right) \tag{Eq. 2}$$

where $T_{air}$ values (°C) are the 30-days smoothed obtained from the MERRA-2 database (3-hours). Figure 11 presents the spatial distribution of the annual mean Tau values in Africa and two local examples of temporal variability in Niger and South Africa.
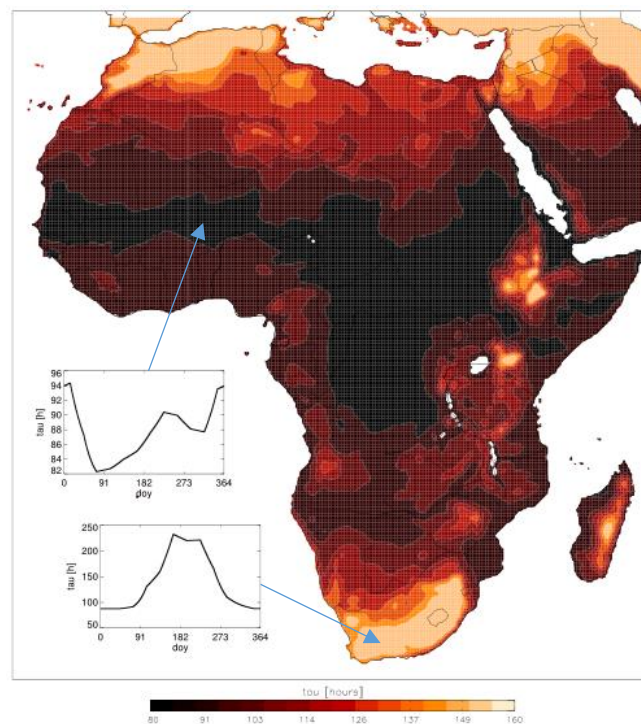


*Figure 11: Annual mean Tau coefficient (in hours) and examples on two selected pixels. Low Tau values (e.g. 80 h) refers to a rapid decrease of the soil moisture, whereas high Tau values (up to 400 h) refers to a slow decrease of the soil moisture.*

## b) Residual soil moisture $\theta_{res}$ and hsoil coefficient maps

The residual soil moisture is the minimal value of soil moisture on a given pixel. Similarly to Tau values, this parameter was determined from residual soil moisture observed at 10 site locations and was found to be related to the presence of vegetation and the air temperature. The formulation can be written as:

$$\theta_{res} = 0.04676 + 0.05936\,(\overline{NDVI}) - 0.00136\,(\overline{Tair}) \qquad \text{(Eq.3)}$$

with $\overline{Tair}$ (in °C) is the annual mean 2m air temperature (source MERRA) and $\overline{NDVI}$ is the annual mean NDVI value provided by ESA-CCI-LC-L4-NDVI (Spot VGT). The $\theta_{res}$ map is shown in Figure 12.

The h$_{soil}$ coefficient (in mm) describes the rapidity of the soil moisture increase during a rainfall event. Over 9 out of 10 sites, a h$_{soil}$ value of 50 mm was found to be adequate compared to *in situ* soil moisture dynamic. However, on the Niger site, a value of h$_{soil}$ equal to 100 mm was required to represent the *in situ* soil moisture dynamic. It was concluded that this parameter can be related to the presence/absence of vegetation. In regions without vegetation, soils are often degraded with an impermeable crust associated with a low infiltration rate. A simple relationship based on mean annual NDVI (ESA-CCI-LC-L4-NDVI) was proposed as :

$$h_{soil} = 120 - \frac{80}{1+178482301e^{(-100*\overline{NDVI})}} \qquad \text{(Eq.4)}$$

Globally, d$_{soil}$ values range from 40 mm (almost everywhere) to 120 mm in arid and semi-arid areas (cf. Figure 12).
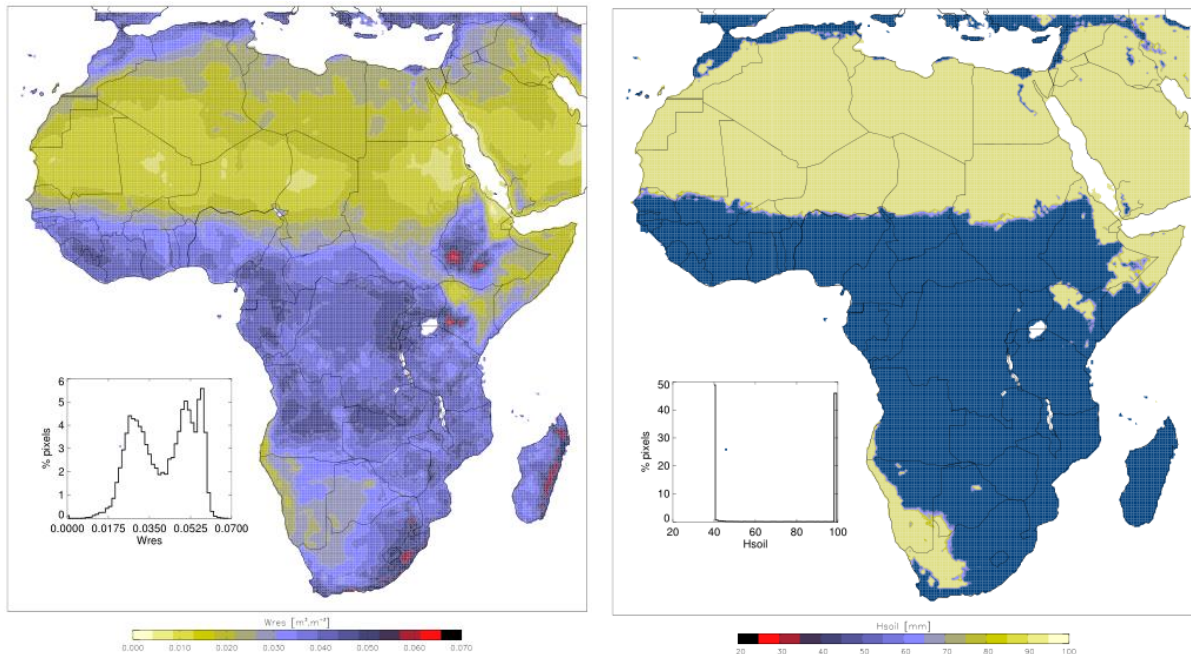


Figure 12: Spatial distribution of (i) residual soil moisture ($\theta_{res}$) and (ii) soil depth (h$_{soil}$)

## c) SMOS CDF-matching coefficients

The CMORPH-Adj reference precipitation products was used to provide a reference soil moisture simulation (2012) with the API model at the African scale. Based on this soil moisture simulation, a calculation of the CDF-matching coefficients (p1 and p2) was made to scale the SMOS L3SM to the reference soil moisture. The scaled SMOS values ($SMOS_{CDF}$) are assumed to be linearly related to SMOS original values as:

$$SMOS_{CDF} = p1 + p2.(SMOS) \tag{Eq.5}$$

with $\qquad p2 = {\sigma_{SMmodel}}/{\sigma_{SMsmos}}$ $\qquad$ and $\qquad p1 = \overline{SM_{model}} - p2.(\overline{SM_{smos}})$

Figure 13 shows the two CDF-matching coefficient maps (p1 and p2) derived from reference soil moisture simulation (based on a reference precipitation product, here CMORPH-Adj) and SMOS measurements. A sensitivity study was done and revealed a strong temporal steadiness of these two maps.
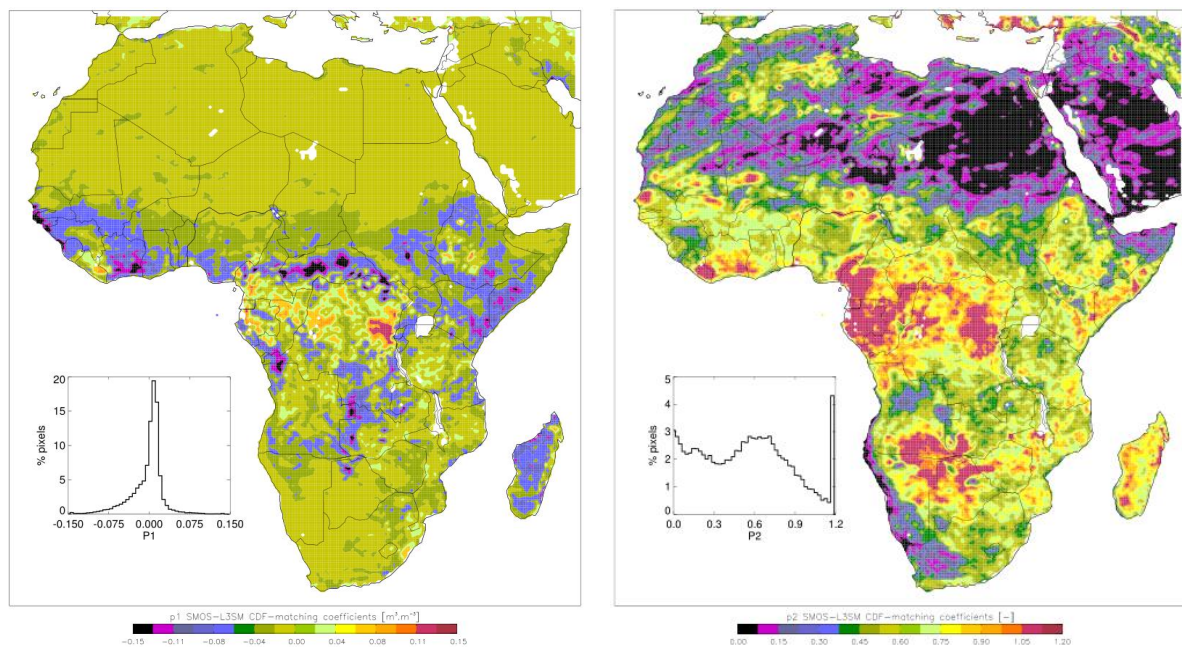


*Figure 13: CDF-matching coefficients (p1(x,y) and p2(x,y) derived from reference soil moisture simulation (based on an Adjusted precipitation product (here CMORPH-Adj 2012)) and SMOS-L3SM CATDS product.*

The CDF-matching coefficients are calculated to remove the bias between SMOS and the reference soil moisture simulation. This step is important to get unbiased SMOS soil moisture estimates as closed as possible to the reference API simulated soil moisture so that the correction of the precipitation can work suitably.

## ANNEX 2 : Potential of the PrISM methodology

The potential of the PrISM methodology depends on the consistency of two signals: the dynamic of the SMOS signal and the dynamic of the API soil moisture simulation. It is possible to map the correlation between these two signals as shown in Figure 14. The correlation ranges between almost zero (in the Sahara desert and Central Africa) to about $R^2=0.7$ in Sahelian regions and Southern Africa. The low correlation in the Sahara desert is due to the weak variation of the two signals (almost no precipitation). In Central Africa, the presence of dense vegetation increases the uncertainty of the SMOS soil moisture estimates. To better illustrate the covariance of the two signals, four pixels are illustrated in Figure 15 (a, b, c, d).
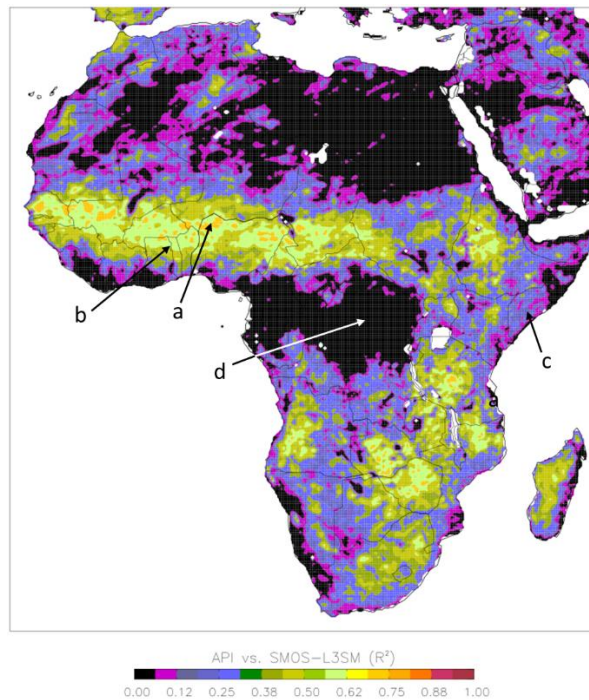


*Figure 14: Annual correlation ($R^2$) between API soil moisture simulation (based on CMORPH-Adj) and SMOS-L3SM soil moisture product.*
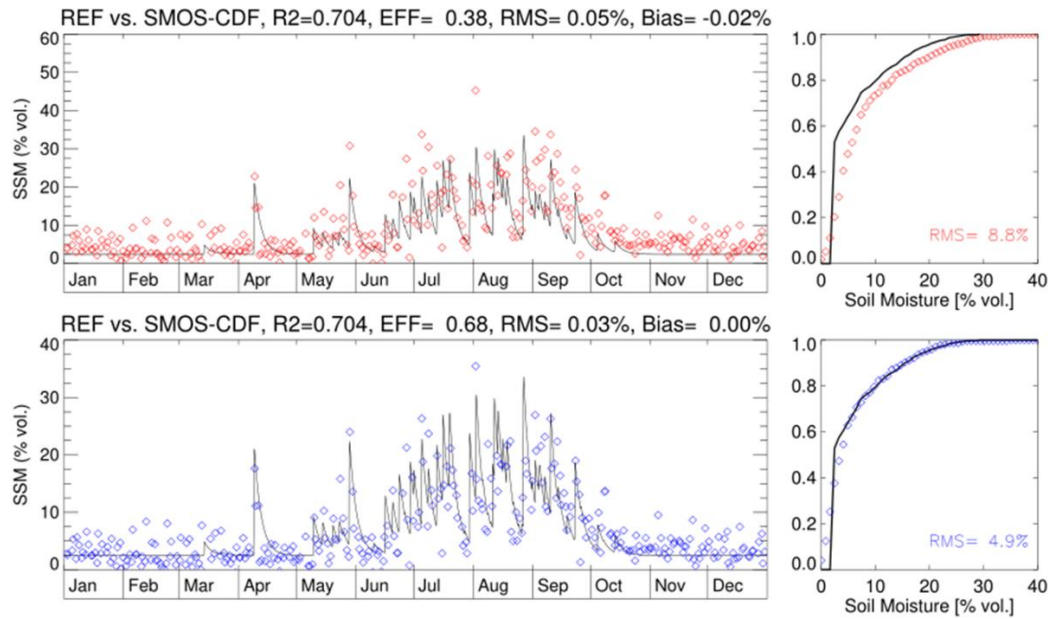
*Figure 15a: (Top) Annual variations of SMOS soil moisture estimates and API soil moisture simulation based on CMORPH-Adj rainfall product in Latitude=12.62N; longitude=5.12E (Northern Nigeria, pixel (a) in Figure 14). (Bottom) same with unbiased SMOS signal after the CDF-matching procedure. The two right graphs show the soil moisture distribution of SMOS and API model.*



*Figure 14b: (Top) Annual variations of SMOS soil moisture estimates and API soil moisture simulation based on CMORPH-Adj rainfall product in Latitude=10.12N; longitude=0.12E (Northern Ghana, pixel (b) in Figure 14). (Bottom) same with unbiased SMOS signal after the CDF-matching procedure. The two right graphs show the soil moisture distribution of SMOS and API model.*
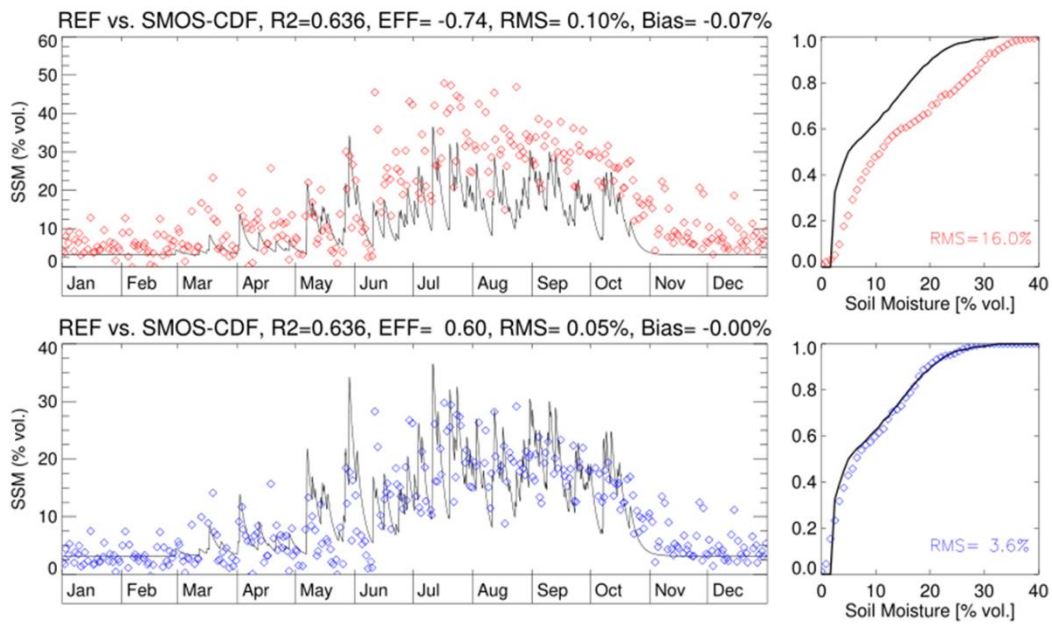
*Figure 14c: (Top) Annual variations of SMOS soil moisture estimates and API soil moisture simulation based on CMORPH-Adj rainfall product in Latitude=2.62N; longitude=45.12E (Somalia, pixel (c) in Figure 14). (Bottom) same with unbiased SMOS signal after the CDF-matching procedure. The two right graphs show the soil moisture distribution of SMOS and API model.*
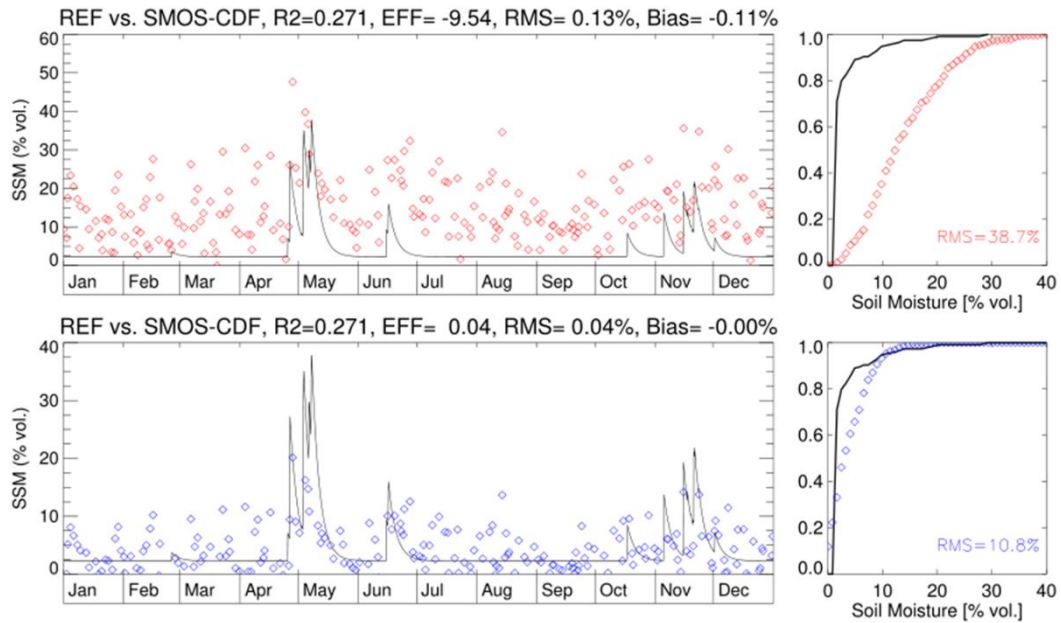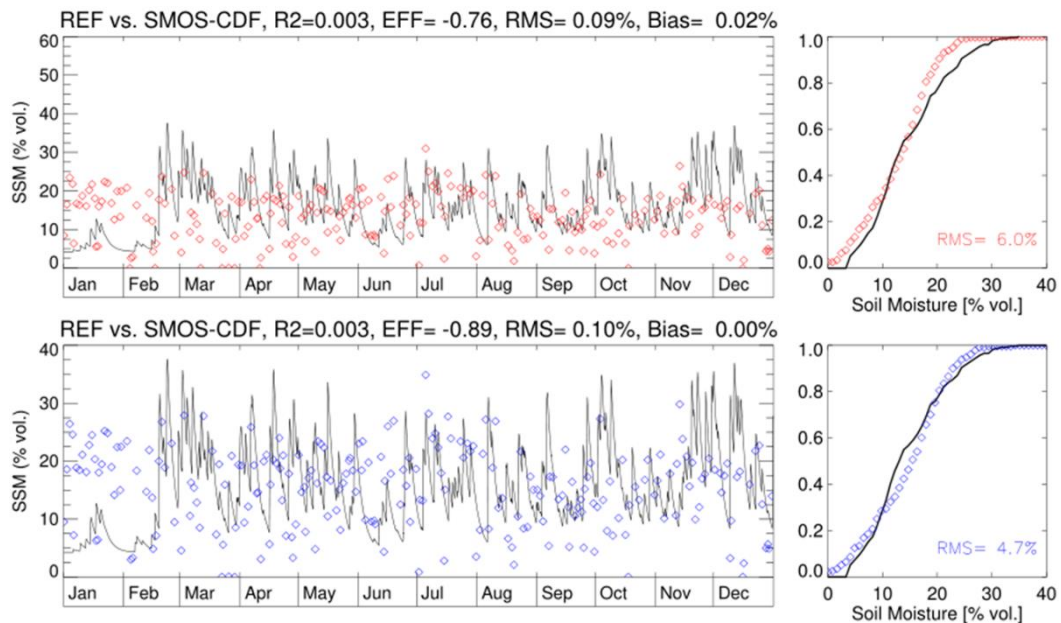


*Figure 14d: (Top) Annual variations of SMOS soil moisture estimates and API soil moisture simulation based on CMORPH-Adj rainfall product in Latitude=0.12N; longitude=25.12E (Democratic republic of Congo, pixel (d) in Figure 14). (Bottom) same with unbiased SMOS signal after the CDF-matching procedure. The two right graphs show the soil moisture distribution of SMOS and API model.*

The four examples shown in Figure 15 (a, b, c, d) gives an overview of various situations. The first one (Sahelian case) is particularly favorable to the PrISM methodology: high correlation score between SMOS and API soil moisture (R²=0.70) and almost perfect match in term of soil moisture distribution after the CDF-matching procedure (bottom right graph, RMS=4.9 % vol.). The second case (Ghana, Figure 15b) presents similar behavior (R²=0.64) and perfect match of the soil moisture distribution

(RMS=3.6% vol.). The third case (Somalia, Figure 15c) presents a relatively weak correlation ($R^2$=0.27) due to a high noise signal during dry periods, and a large mismatch in the soil moisture distribution (RMS>10 % vol.). Finally, the fourth case (Central Africa forest) shows a very low correlation ($R^2$=0.003) but a relatively good soil moisture distribution (RMS=4.7 % vol.).

## ANNEX 3 : Files structure

The files are in netcdf format. The structure is given below (ncdump –h UNIX function)

```
dimensions:
      latitude = 297 ;
      longitude = 285 ;
      time = 2920 ;
variables:
      float latitude(latitude) ;
             latitude:long_name = "latitude" ;
             latitude:standard_name = "latitude" ;
             latitude:units = "degrees_north" ;
             latitude:axis = "Y" ;
      float longitude(longitude) ;
             longitude:long_name = "longitude" ;
             longitude:standard_name = "longitude" ;
             longitude:units = "degrees_east" ;
             longitude:axis = "X" ;
      float rainfall(time, latitude, longitude) ;
             rainfall:long_name = "Precipitation amount" ;
             rainfall:units = "mm" ;
             rainfall:_FillValue = -9999.f ;
             rainfall:valid_max = 110.7814f ;
             rainfall:valid_min = 0.f ;
      float rainfall_error(time, latitude, longitude) ;
             rainfall_error:long_name = "Precipitation amount error" ;
             rainfall_error:units = "mm" ;
             rainfall_error:_FillValue = -9999.f ;
             rainfall_error:valid_max = 7387.573f ;
             rainfall_error:valid_min = 0.f ;
      int time(time) ;
             time:long_name = "time" ;
             time:standard_name = "time" ;
             time:units = "seconds since 1970-01-01 00:00:00 utc" ;

// global attributes:
             :Conventions = "CF-1.5" ;
             :title = "Rainfall amount 0.25 x 0.25 degrees / 3 h, from Pellarin et
al 2013 algorithm with SMOS assimilation (Particle Filter)" ;
             :institution = "IGE (Institut des Geosciences de l Environnement),
Grenoble, FRANCE" ;
             :history = "Tue Mar  6 16:22:54 2018" ;
             :Configuration1 = "CDF-Matching coefficient (p1,p2) obtained on 2012
(CMORPH-Adj)" ;
             :Configuration2 = "RFI and DQX thresholds are 0.4, 0.05" ;
             :Configuration3 = "Initial precipitation product : CMORPH-Raw (0.25deg,
3h)" ;
             :references = "Roman-Cascon, C., Pellarin, T., Gibon, F., Brocca, L.,
Cosme, E., Crow, W., Fernandez, D., Kerr, Y. and Massari, C. Correcting satellite-
based precipitation products through SMOS soil moisture data assimilation in two land-
surface models of different complexity: API and SURFEX, Remote Sensing of Environment,
200 (2017) 295.310" ;
```